UCRL- 89316 - Rev. 1
PREPRINT

STATIC AND DYNAMIC ANALYSES ON THE MFTF-B VACUUM VESSEL

Dorothy S. Ng

This paper was prepared for submittal to the
10th IEEE Symposium on Engineering Problems
of Fusion Research, Philadelphia, PA,
December 5-9, 1983.

January 15, 1984

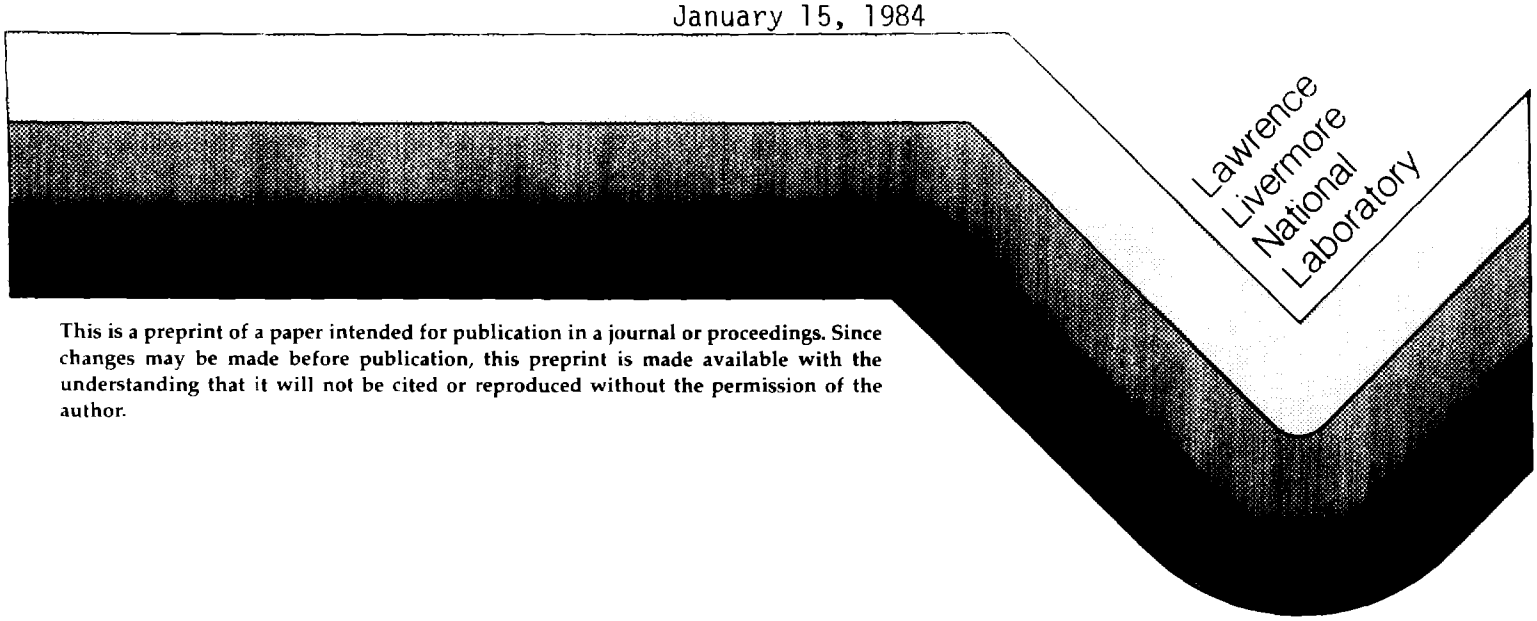

STATIC AND DYNAMIC ANALYSES ON THE MFTF-B VACUUM VESSEL*

Dorothy S. Ng

Lawrence Livermore National Laboratory, University of California
Livermore, CA 94550

ABSTRACT

The Mirror Fusion Test Facility is a major magnetic fusion energy project at the Lawrence Livermore National Laboratory. An important component of this facility is the vacuum vessel, which forms the vacuum chamber. The vessel is supported on twenty-two pairs of legs that rest on reinforced concrete piers. In performing static and dynamic analyses on the vacuum vessel, we separately investigated the load distribution under gravity loads, pressure loads, electromagnetic loads, and thermal loads. We also performed sophisticated dynamic analyses to predict the structural behavior under a postulated earthquake. The modeling assumptions and analytic procedures are highlighted in this paper.

---

*Work performed under the auspices of the U.S. Department of Energy by the Lawrence Livermore National Laboratory under contract number W-7405-ENG-48.

INTRODUCTION

The Mirror Fusion Test Facility (MFTF-B) at Lawrence Livermore National Laboratory (LLNL) is a large-scale tandem mirror fusion experiment. In the magnetic fusion concept, a fusion reaction is created by injecting beams of energetic neutrals into a high-temperature plasma. Magnetic fields confine the plasma in a vacuum chamber. The magnetic fields are provided at each end by a tandem mirror cell, which contains a pair of C-shaped magnets called the yin-yang pair. The central cell of the plasma chamber has a solenoidal magnetic field. The vacuum environment serves to minimize heat conduction from the high-temperature plasma. The vacuum pressure in the cylindrical vessel is maintained by a pumping system.

The MFTF-B (including the vacuum vessel system) was designed and built to accommodate experiments with maximum magnetic fields of 12 tesla. To aid in comprehending the structure's behavior, we performed static and dynamic analyses on computer models for the axicell magnets and vacuum vessel, simulating various loading conditions and seismic criteria. (A movie animating model deformation and mode shapes also was made to depict the behaviour of the structure). This paper is a report of these analyses and the results.

REASONS FOR ANALYSES

A detailed computer model for use in comprehensive design analyses was generated by Pittsburgh-Des Moines Corporation (PDM), who hold the contract for vacuum vessel design. An independent analysis on the vacuum vessel (which is reported here) was performed by LLNL for the following reasons:

- To monitor the PDM engineering design.
- To compute the hanger loads and foundation loads for the corresponding design contractors.
- To provide seismic responses of the magnets and vessel for design of attached equipment.
- Additional analyses verify modeling assumptions.

GEOMETRIC CONFIGURATION OF MFTF-B

A horizontal cylindrical shape was chosen for the vessel in order to effectively maintain a vacuum environment. Longitudinal stiffeners carry longitudinal loads to the adjacent ring stiffeners, which in turn transfer the loads and the magnet weight downward to the legs.

Modules

The central cell of the plasma chamber, which houses the solenoid magnets, is a cylinder 26 feet in diameter and 72 feet in length. The cylinder is constructed of eight sections (six of which are modular), contains 18 ring stiffeners, and is supported on 14 pairs of legs (see Fig. 1). Six of them are removable. Additionally, the cylinder is strengthened by four longitudinal stiffeners and 36 small reinforcing bars.

The cylinder is connected to the tandem mirror end plugs (yin-yang cell) by a 45-degree divergent transition cone. Each end-plug cylinder is 35 feet in diameter and 65 feet long, is reinforced by four ring stiffeners and eight longitudinal stiffeners, and is supported on four pairs of legs. Because of the heavy tandem mirror coils, the inner ring stiffeners and legs are in double sections. It has four spherical beam domes, and the end plugs are capped by a spherical end dome.

The vessel, legs, and support-box beams are built of nonmagnetic stainless steel (304). The support frames at the central cell are built of carbon steel. The central cell is allowed to bear on a shear wall at the middle of the structure. The end-plug legs are welded and grouted to four reinforced concrete piers, each having a cross section of 10 by 13 feet. All vessel support structures are placed on a group of 4-foot-thick mat foundations.

Penetrations

To provide access to the inside of the vessel, numerous circular and rectangular penetrations are scattered over the vessel shell. Beam lines, cooling systems, diagnostics, and other types of equipment are connected through the penetrations. Some superstructures, such as platforms and stairways, are also built onto the vessel.

Magnets

Inside the vessel, 42 superconducting magnets are suspended by vertical hangers and side struts that are connected directly to the ring stiffeners. Drag struts are tied to longitudinal stiffeners that bridge over two adjacent ring stiffeners. The magnets are contained in five modules and are linked by longitudinal struts.

The complete magnet system consists of two pairs of C-shaped tandem mirror coils (EM2, EM1, WM2, WM1), two pairs of C-shaped transition coils (ET2, ET1, WT2, WT1), two sets of eight trim coils (ETR1 to ETR8, WTR1 to WTR8), two sets of three axicells (EA2o, EA2i, EA1 and WA2o, WA2i, WA1), and 12 solenoids (ES6 to ES1, WS6 to WS1). The M2, M1, and T2 magnets are in the end-plug modules; T1, A2o, A2i, A1, and S6 magnets are in the axicell modules, and the rest of the solenoids are in the central-cell module. Some of the solenoids are tied in pairs by box beams. The trim coils are grouped in fours. Each group is hung on the T2 or T1 magnets.

MODELING ASSUMPTIONS

To realistically model this complicated system, we made certain assumptions in order to simply the computer model and, at the same time, retain an adequate representation of the structure.

Symmetry

The vacuum vessel, the support structures, and the magnet system (except for the C-shaped magnets) are symmetrical with respect to the vertical median plane. As the exception, the west C-coils are rotated 90 degrees about the longitudinal axis relative to the east C-coils. The hangers and struts are symmetrical except for the drag struts on the yin-yang cell and those on the solenoid module, which has only one group of drag struts. These drag struts span the plane of symmetry from the west solenoid WS1 to the east-vessel shell.

Even with these unsymmetrical entities, we make the assumption that the system is symmetric to the midplane and we include only the west half of the structure in the computer model. We must modify the solenoid-module drag struts by turning them backward. We assume they are connected to the west-vessel shell and cross the face of symmetry to the position of the east solenoid ES1. Because the east half is not modeled, the drag struts are tied rigidly back to the west solenoid WS1.

The solenoid-module drag struts carry heavy longitudinal loads to the vessel shell. Consequently, in the real structure, the first module of the east central cell is strengthened to resist these heavy loads. In the model, this first east module (and its corresponding support legs and foundations) replaces the first west module of the central cell.

Boundary Conditions

The boundary conditions at the face of symmetry restrain the longitudinal (east-west) translation as well as the rotations about the vertical (up-down) and transverse (north-south) directions. These boundary conditions apply to most loading conditions except for the magnet fault-loading and longitudinal seismic loading.

The solenoid-module drag struts are attached to the vessel at a point 49 inches west of the face of symmetry. Under longitudinal magnetic forces, this 49-inch ring of shell is heavily loaded because of longitudinal restraint at the face of symmetry. (This high-stress phenomenon does not exist in the real structure). Because this is an unsymmetric loading condition, symmetric boundary conditions are inappropriate. To simulate the true situation, we replace the symmetric boundary condition in the longitudinal direction with a series of translational springs. We apply these longitudinally at the face of symmetry to model the stiffness of the missing east half of the vessel.

For dynamic analyses, symmetric boundary conditions apply to transverse and vertical excitations. For longitudinal excitation analysis, antisymmetric boundary conditions are enforced. This allows the model to translate in the east-west direction and to rotate about both axes in the mid-vertical plane.

The base-support boundary conditions of the system depend on the relative flexibility of the support structures with respect to the 4-foot-thick foundation upon which the system sits. At the plug cells, the rotational stiffness of the massive concrete piers is much greater than that of their foundations. Obviously the foundation can be driven to rotate by the piers. This foundation flexibility considerably affects the load distribution between the end plug and the central cell. We must apply a transverse rotational spring beneath each pier to simulate the foundation flexibility.

For the central-cell support structures, the bases of columns and knees are assumed to be fixed supports. The supports are restrained from all translations and rotations. Close to the face of symmetry, the system rests

on a shear wall. Since the shear wall is not designed to carry any additional lateral forces or moments from the vessel, the support points are fixed against vertical translation only.

Element Types

The vessel shell and support legs are modeled by four-node, quadrilateral, thin, plate/shell elements. This element type is capable of handling in-plane and out-of-plane loadings. Most of the plate elements have an aspect ratio that is less than 1 to 5.

We model the stiffeners and support-leg flanges by using two-node, prismatic, three-dimensional beam elements. Because the shell and beam elements share common node points, the offset effect of the stiffeners and ribs must be included. To compensate for this offset effect, we add a portion of the shell to the calculation of the moment of inertia about the major neutral axis of the stiffener or rib.

The superconducting magnets are composed of the conductor bundles, coil cases, and thermal shields. The coil case is made from nonmagnetic stainless steel (304 LN) and provides most of the stiffness in the magnet. The beam elements representing the magnets include only the stiffness of the magnet cases. However, the total weight of the magnet, including the support hangers, is uniformly distributed in the beam weight and mass densities. Because the trim coils are small and attached on transition magnets T2 and T1, only their weights are included as concentrated loads.

The hangers and struts are designed to be two-force members because the monoball connections are pinned joints. In the input data for the geometric properties of the beam elements, a very small value is used for the shear areas and moments of inertia. This technique is used to simulate the truss-like action of the hangers and struts.

Two types of boundary elements (springs) are used in this model to implement the boundary conditions. Rotational springs are applied at the midplane of the foundation, beneath the piers, to represent the foundation rotational flexibility. The stiffness of these springs is calculated by the formula published in Ref. 1.

The other type of boundary elements are translational springs that are applied longitudinally at the face of symmetry. Their function is to capture the resultant forces at the face of symmetry of the model. These resultant

forces should balance the support loads and applied loads in an equilibrium check.

External Loads

The vacuum vessel is capped at both ends by an end dome. The end dome is hung on the vessel periphery on four major supports, which together with four pins serve to stabilize in case of earthquake The end dome does not provide any radial stiffness to the vessel shell and, therefore, is not included in the model. By design, the total weight of the end dome is carried by the top two supports on the vessel.

The end dome is pressed tightly on the vessel periphery when the vessel is under vacuum pressure. Therefore, for dynamic analysis, we uniformly distribute the end-dome mass along the periphery in all three directions of excitation.

Numerous types of auxiliary equipment are installed on the vessel. Their weights are uniformly distributed over the shell within the corresponding regions. The plate densities are adjusted to include these equipment weights. Two 6000-pound beam-injector loads are applied as concentrated loads on the top beam dome. Equipment weighing over 6,000 pounds will be supported off the vessel by space frames.

Finite-Element Parameters

The model is reasonably simplified. For example, the double ring stiffeners and the double legs are represented by one group of beams and plates. The beam dome covers are simply connected to the stiffeners. Nodes are created only for the stiffener, hangers, drag struts, and beamline locations (see Fig. 2). The module joints are not described in this model.

Longitudinally, we use 19 elements to model the vessel shell and stiffeners. Their lengths are defined by the locations of the ring stiffeners and beamline locations. For modeling, we use a total of 24 elements for the ring stiffeners and 24 elements for each magnet. Node coordinates are assigned to satisfy the hanger and drag-strut locations.

Most components (such as the hangers, magnets, and support systems) are modeled at their center lines by beam elements. In the real structure, the component connections are at their outside edges. In the model, rigid links are used to tie elements together. These links are beam elements with large

areas and moments of inertia, so that they effectively are relatively rigid compared to the other elements of the model.

We constructed the model by using 1357 node points, 1610 beam elements, 598 plate elements, and 28 spring elements. The model contains over 7300 degrees-of-freedom. and its half-bandwidth is 516 equations. The model is analyzed statically and dynamically on the basis of loading conditions and local seismic criteria.

STATIC ANALYSES

The system is under various types of loads. To better understand the model behavior, loads are applied separately to the model. The following load cases are defined to satisfy requirements of the magnetic fusion experiments.

Gravity Load

Gravity load includes all internal-element weight and external auxiliary-equipment weight. A magnet load of 1340 kips (1000-lb units of deadweight) is suspended on the stiffeners, and a load of 550 kips of auxiliary-equipment weight is distributed over the shell. The vessel and legs weigh over 1000 kips. Including the piers and the support frames, the total weight is over 4000 kips.

Vacuum Pressure Load

The vessel model is subjected to vacuum pressure along with the vessel magnetic force. A unit pressure of 16.2 lb/in^2 is applied normal to the vessel shell. The end dome is not included in the model. The vacuum pressure from the end dome is applied uniformly as concentrated loads on the node points at the periphery of the shell.

Magnetic Load Under Normal Operation

At the same time the magnets generate a magnetic field for plasma confinement, they also produce large magnetic forces. When the magnets are fully in operation, the magnetic forces are defined as the magnetic load case under normal operation. The radial magnetic forces in each magnet are self-balanced. In the whole magnet system, the longitudinal forces are also in equilibrium. However, within one-half of the magnet system, those

longitudinal forces are cumulative. The longitudinal forces from each module are transferred to the vessel by drag struts.

Fault Magnetic Load

In case of emergency, different magnets could be in a fast dump condition. The change of electric voltage can induce eddy current in adjacent magnets. In these fault cases, the magnetic forces produced by the magnets are quite different from those produced under normal operation. A magnetic load matrix is generated to identify the fault cases. The worst fault case is adopted as the fault magnetic load.

Environmental Thermal Load

The MFTF-B system is surrounded by a 7-foot-thick vault wall, and the expected environmental temperature variation of the system is $\pm 10^{o}F$. In the model, the whole system is warmed by $10^{o}F$.

In the computer model the truss elements, but not the beam elements, are capable of handling thermal stresses. Therefore, a group of truss elements are superimposed on all beam elements. The truss elements effectively take care of the axial forces, and the beam elements resist the shears and moments.

Cool-Down Thermal Load

The superconducting magnets are operated at cryogenic temperature but the vessel remains at room temperature. The hangers and struts are at room temperature at the vessel end but are at 4 degrees kelvin (K) at the magnet end. The magnet support system is designed to avoid lock-in thermal stresses. To verify this, a cool-down thermal load is applied to the model. The vessel is kept at room temperature, the magnets at 4 K, and the magnet support elements at the average temperature of the vessel and magnet. An equivalent coefficient of expansion for the support element is computed on the basis of its real thermal contraction.

DYNAMIC ANALYSES

The vessel system is designed to resist a postulated seismic incident at the LLNL site. For the computer model, we analyze the response spectrum for specified seismic motions. To do this, we first extract the dynamic

characteristics of the computer model, such as nodal masses, eigenvalues (frequencies), and eigenvectors (mode shapes). The high-frequency modes are truncated and the modal responses are computed. The structural response is the summation of all computed modal responses in the model. The summation is obtained by the square root of the sum of the square (SRSS) method. Because earthquake motion can occur in any direction, we excite the model in three global directions and again combine the responses by the SRSS method.

Design Response Spectrum

The input spectrum for the LLNL site was based on time histories of an ensemble of West Coast earthquakes. This site-specific spectrum (see Ref. 2) has a zero-period acceleration (ZPA) of 0.25 g and is applied in the two horizontal excitations. For vertical excitation, the ZPA is scaled by two-thirds.

We performed dynamic analyses on a fixed base model. Several analyses of soil-structure interaction also were performed on the vessel system along with its surrounding vault wall by Structural Mechanic Associates (SMA). Compared to a fixed base analysis, the SMA results led to a 25% reduction in ZPA, which is caused by a combination of soil damping and soil-structure interactions. Based on this finding, we reduced the horizontal ZPA to 0.19 g but left the vertical ZPA at 0.17 g.

Damping Coefficient

For the design spectrum we selected 5% damping. Although the vessel is made of stainless steel, it rests on massive reinforced-concrete piers and foundations. A series of dynamic excitation tests performed on the end-plug vessel indicates the 5% damping coefficient is reasonable. In the tests the vessel response to an impulsive input function was measured at different locations. Frequencies and damping values are extracted for each mode by the Fourier Theory. The average computed damping value indeed is close to 5%. At 5% damping, the peak spectral value is 0.59 g at a period of 0.33 s, tapering down to 0.14 g at 2 s.

Modal Truncation

Theoretically, a computer model has as many mode shapes as its degrees of freedom. Generally, the first few (or low-frequency) modes extracted will

dominate the structural response because of its being magnified by their high participation factors and spectrum accelerations. The high-frequency modes have less effect in magnifying the structural response.

A technique for ensuring adequate seismic design is included in the document "Recommended Revisions to Nuclear Regulatory Commission Seismic Design Criteria" (see Ref. 3). The document recommends a modal truncation cutoff frequency of 33 hertz and recommends a modal participating mass equal to 90% of the total structural mass. If less than 90% of the mass is captured, the remaining mass should be accounted for by static analysis.

Because the modal extraction is a time-consuming process on the computer, we only extract 60 of the total number of modes possible. The last mode extracted is close to 33 hertz. The effective modal masses are computed for all 60 modes. From these, the first 40 modes with the highest effective modal mass values are selected for the response spectrum analyses.

Computer Programs for Analyses

As described previously, the procedure for the response-spectrum analysis is quite complicated. Program SAP4 (see Ref. 4) is a well-developed structural analysis program for linear elastic, static, and dynamic analyses. We use SAP4 for static analysis (which takes 15 minutes to complete on the CDC-7600 computer) and also in dynamic analysis for setting up the stiffness and mass matrices and the element connectivity array. For modal extraction, we use SUBSP, which uses a subspace iteration algorithm with shifting to solve the eigenvalues and eigenvectors. For modal truncation, we use MODPAR to select the modes that have the highest modal participating mass. We use RESPAN for structural responses and SRSS to sum the responses. The use of these programs is illustrated in the flow chart of Fig. 3. Modal extraction is the most time-consuming process in dynamic analysis, roughly 70 minutes of computer time being needed to extract 50 mode shapes.

EVALUATION OF ANALYSES

The resulting loads from LLNL are compared with the results of PDM, which are evaluated for adequacy of the structural members. All static load conditions are processed separately so that we can understand the behavior of the model under each condition. This is also helpful in qualifying the

model. For evaluation purposes, results from different load conditions must be combined to obtain the worst case.

Load Combination

The load cases considered are the following: gravity (G), vacuum pressure (V), normal operation magnetic force (Mn), fault magnetic force (Mf), environmental thermal (Te), cool-down thermal (Tc), and earthquake (E).

The operation sequence during the experiment is first to evacuate the vessel and then to cool down the magnets before energization. The magnetic-force load cases Mn and Mf do not occur simultaneously. The higher load of these two cases is selected for the load combination. The Tc load case happens before magnet energization; the Te load case exists year round; and the probability of the E load case occurring is relatively low. Both Te and E can produce either tension or compression on components. To obtain the worst possible case, we define five realistic load combinations as follows:

(1) G

(2) $G + V$

(3) $G + V + M \pm Tc$

(4) $G + V + M \pm Te + Tc$

(5) $G + V + M \pm E + Tc$

The combined-element loads are compared to the allowable stress to determine adequacy.

Allowable Stress Criteria

The allowable stress criteria are defined in the ASME Pressure Vessel Code Section VIII. The components are divided into pressurized components (vessel and stiffeners) and nonpressurized components (legs and supports). Stresses are identified as either primary or secondary. Because of the low incidence of earthquakes, a lower safety margin is applied in the earthquake case.

Model Deformation

The mirror fusion experiment demands high precision with respect to magnet locations. The test facility is designed for minimum deflection under

static loads. The largest computed vertical deflection is 0.25 in. at the transition T2 magnet. On the vessel, the largest vertical deflection is 0.19 in. at the vertical hanger-attachment point at the T2 magnet. The top of the west end of the vessel is displaced longitudinally a total of 0.15 in. from the sum of all static load cases.

Dominant-Mode Shapes

In the transverse and longitudinal directions, the dominant modes are at frequencies of 3.88 and 4.38 hertz, respectively, and the total effective mass included is 75% and 88%, respectively. In the vertical direction, the dominant frequency is at 6.75 hertz. From vertical excitation of the 40 most dominant modes, the effective mass amounts to only 54% of the total. A pseudostatic analysis is performed on the transverse and vertical excitations to account for the remaining mass.

In transverse excitation, the yin-yang module shows the largest mode shapes in the first mode. The solenoid and axicell modules show the most motion in rotation in the second mode. (This is seen in Figs. 4 and 5, where the dots in the figures indicate the original shape.) In vertical excitation, the dominant mode also has high rotational motion in the axicell module (see Fig. 6). This indicates a dynamic coupling effect in the model. In the longitudinal direction, the model exhibits a rigid-body-like motion (see Fig. 7).

The input spectrum has a peak spectral acceleration at about 3 hertz. The frequencies of the dominant mode of the model are close to the peak spectral acceleration, which results in an overall equivalent acceleration factor of about 0.56 g at the base. The upper part of the model has higher magnification because it is amplified by its weight.

Magnet Hanger Loads

The magnet static behavior is as expected. In the gravity load case, the magnet weights are supported by the vertical hangers. In the axicell and central-cell modules, the moments created by the eccentric loads are resisted by the drag struts and the corresponding vertical hangers. The longitudinal magnetic loads are transferred to the vessel by the drag struts only. Vacuum pressure does not produce any load in the magnet supports. The support arrangement is designed to avoid any lock-in thermal load and, indeed, there is only a small load resultant in both of the thermal load cases analyzed.

The total dynamic loads are obtained by combining the results from three excitation directions. The dynamic load resultants in magnet supports are higher than expected. Under vertical excitation, the transverse struts carry significant loads. During transverse excitation, the vertical hangers resist significant loads. The high dynamic loads are thought to be caused by the dynamic coupling effect occurring between vertical and transverse directions. The same dynamic coupling effect was observed in the PDM model.

Vessel Foundation Loads

Of the total weight, 81% is supported by the end-plug piers, 14% by the support frame of the central cell, and the remaining 5% goes to the shear wall. The vacuum-pressure load produces a small vertical load in the piers and support columns and produces slightly more than 100 kips of longitudinal shear in the plug foundation. The magnetic load and the environmental thermal load produce less than 100 kips vertical load in the piers and columns and less than 200 kips longitudinal shear in the plug foundation. The central-cell foundations receive insignificant shear from these load cases. The cool-down thermal load case does not produce any load in supports or foundations.

The results of the dynamic analyses indicate an equivalent acceleration level of 0.4 g in the plug and over 0.5 g in the central cell. Overall and except for the piers, the design of the vessel support system is dominated by the dynamic loads. Because of the additional flexibility from the plug foundation springs, more load is shifted to the central cell during longitudinal excitation. As a result, the vertical dynamic forces in the central-cell columns are much bigger than the gravity load forces. This indicates the necessity for further investigation of foundation springs.

CONCLUSIONS

The results of two independent analyses by PDM and LLNL are comparable. Generally our findings from static analyses were as expected, while some of the dynamic magnet-support loads found were higher than expected. Analyses by both PDM and LLNL showed this same phenomenon. It is believed that the highly complicated model experiences some dynamic coupling effects. The analyses have, in general, verified the adequacy of the design approach used.

The shifting of the foundation load by the plug-foundation springs indicates the sensitivity of foundation loads to flexibility of the central-cell foundation. This will be further investigated.

At the time these model analyses of the MFTF-B Axicell vessel were performed, magnetic forces for the trim coils were not yet available. These additional magnetic forces, as well as misalignment loads on the magnet that are caused by manufacturing tolerance, dictated the need for larger stiffeners in the vessel. Therefore, we revised the model. Complete static and dynamic analyses are being performed on the retrofit model to ensure the adequacy of design.

REFERENCES

[1] M. Hetenhi, "Beams on Elastic Foundation," in University of Michigan Studies, Scientific Series, (The University of Michigan Press, Ann Arbor, Michigan, 1946), Vol. XVI.

[2] J. A. Blume and Associates, Engineers, Investigation of Faulting at Lawrence Livermore Laboratory, Lawrence Livermore National Laboratory, Livermore, Calif., UCRL-13568 (1972).

[3] D. W. Coats, Recomended Revisions to Nuclear Regulatory Commission Seismic Design Criteria, Lawrence Livermore National Laboratory, Livermore, Calif., NUREG/CR-1161 (1979).

[4] S. J. Sackett, Users Manual For SAP4, Lawrence Livermore National Laboratory, Livermore, Calif., UCID-18226 (May 1979).

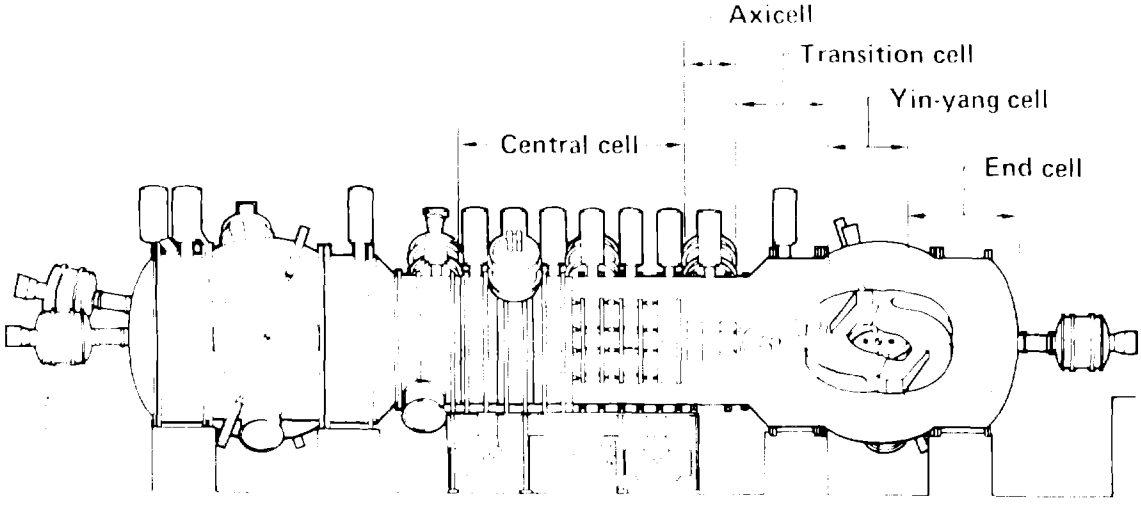

Figure 1. Configuration of magnets and vessel of MFTF-B Axicell. Right half is cutaway section to show interior components.

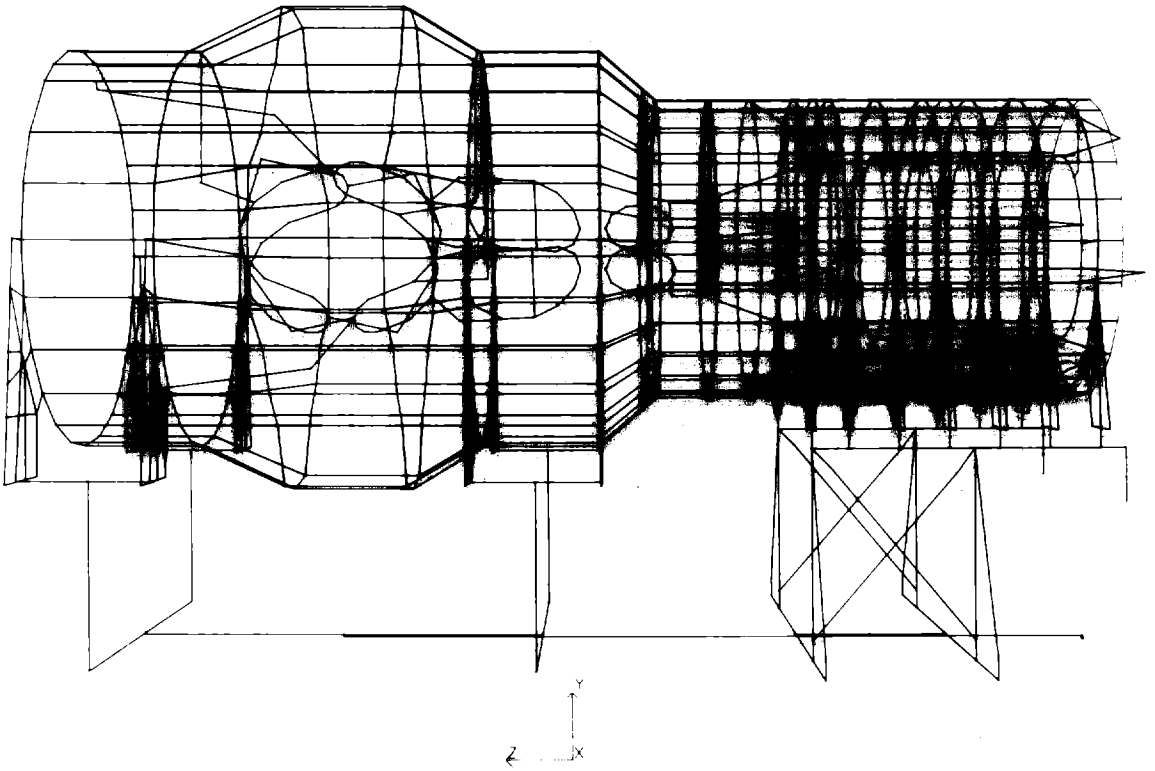

Figure 2. Computer model of magnet and vessel systems of MFTF-B Axicell.

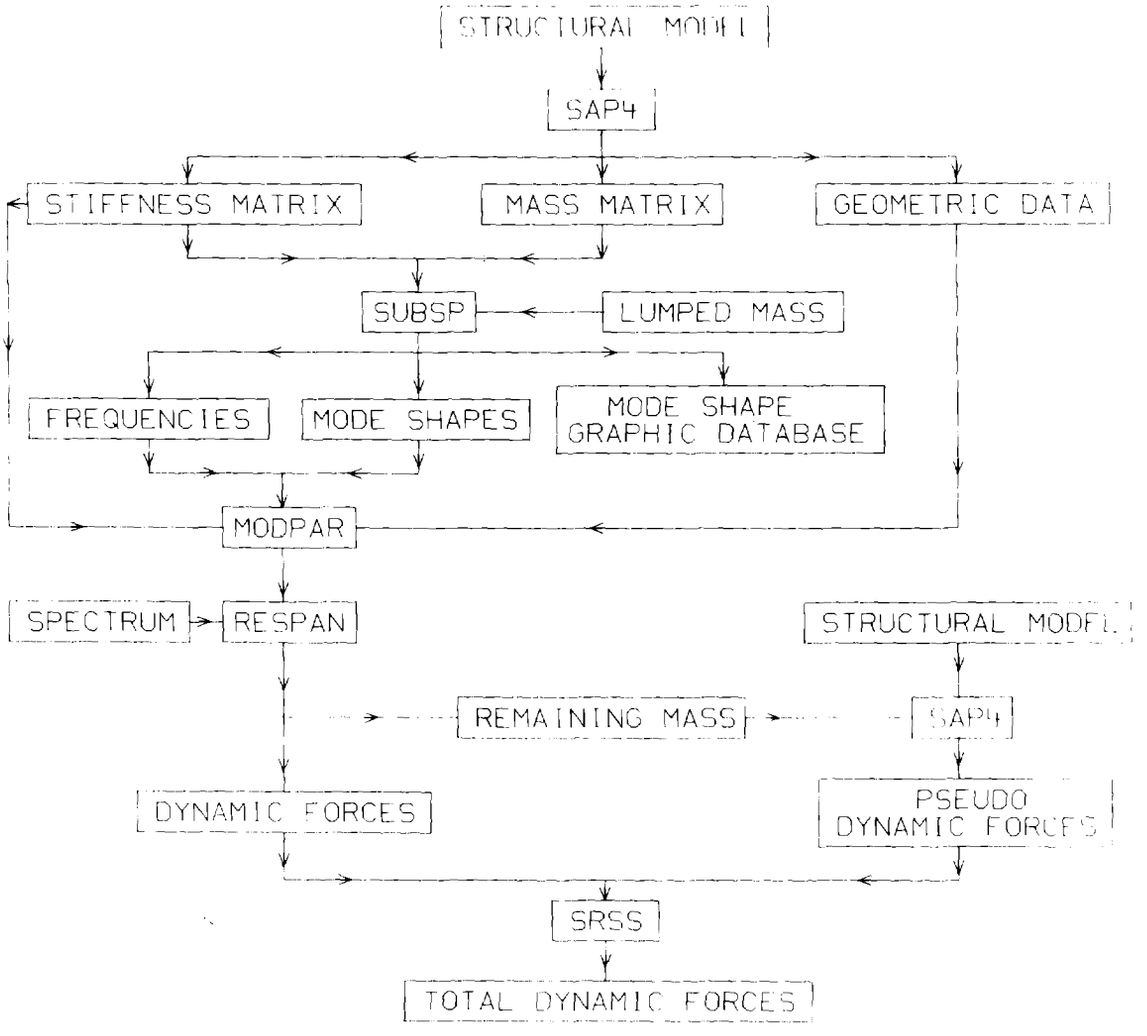

Figure 3. Flow chart for dynamic analysis.

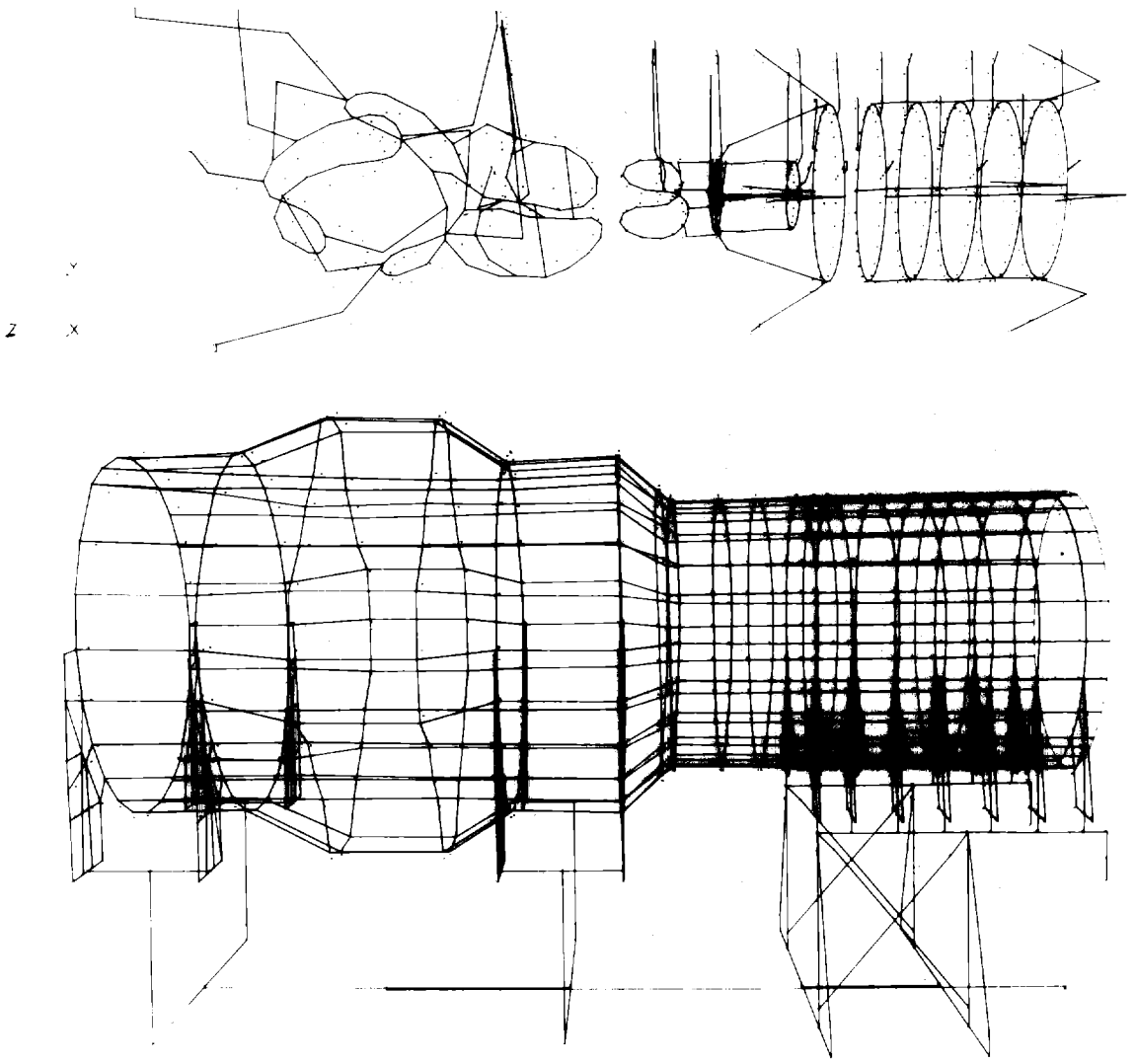

Figure 4. Computer model of magnet and vessel systems of MFTF-B Axicell: Transverse dominant-mode shape at 3.88 hertz, modal participating mass of 41.1%, and scale factor of 150.

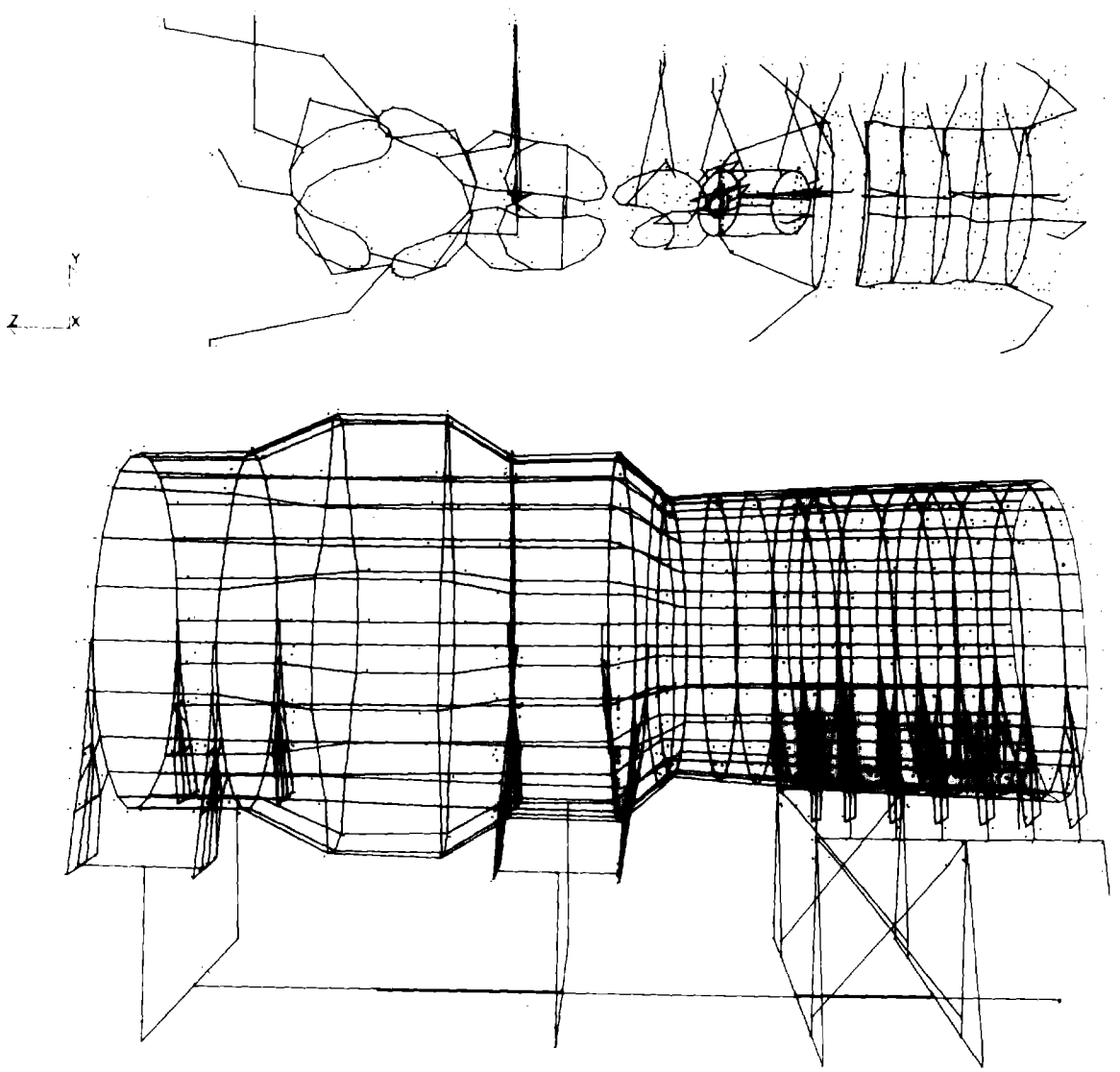

Figure 5. Computer model of magnet and vessel systems of MFTF-B Axicell: Transverse dominant-mode shape at 5.15 hertz, modal participating mass of 11.6%, and scale factor of 150.

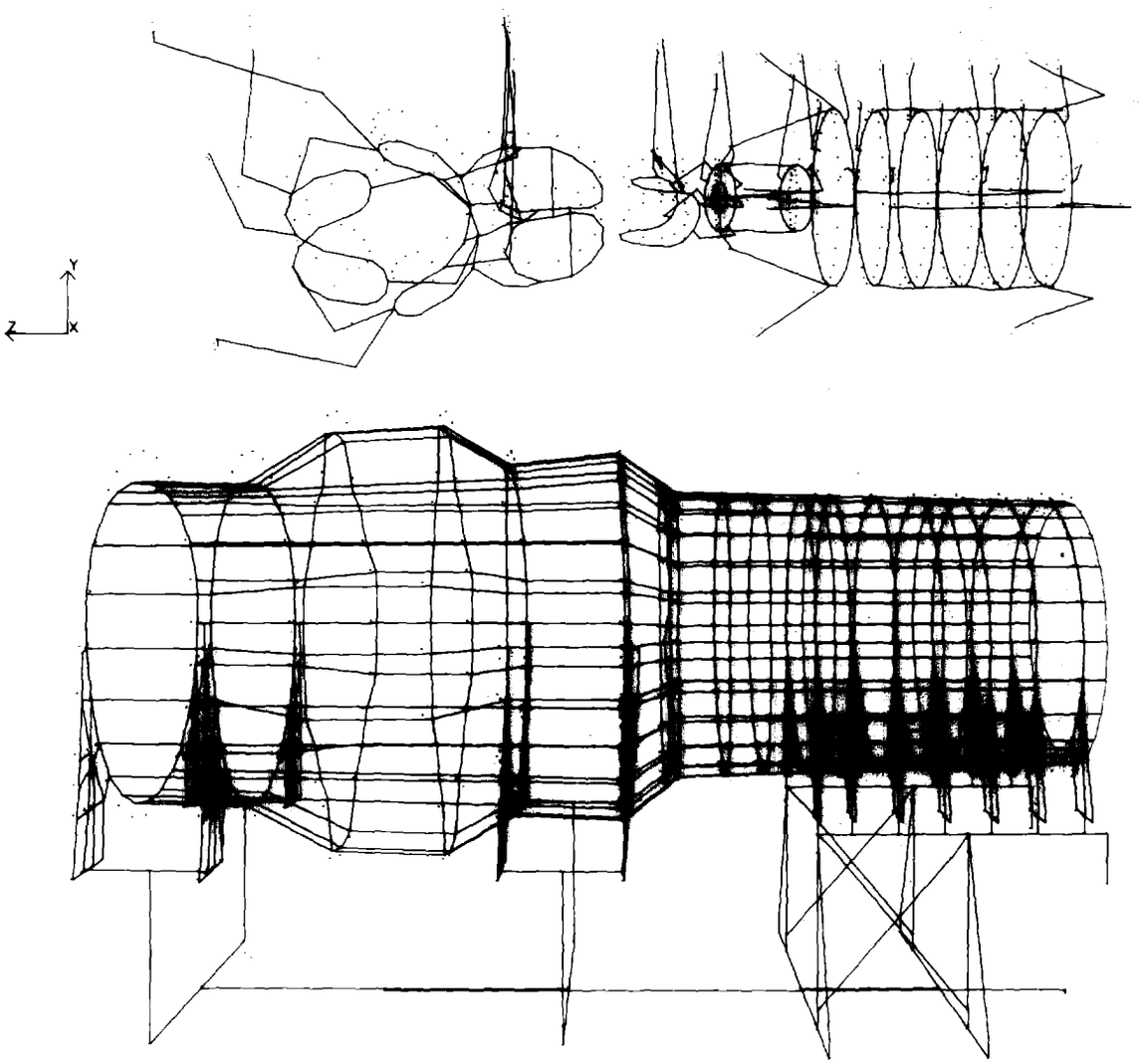

Figure 6. Computer model of magnet and vessel systems of MFTF-B Axicell: Vertical dominant-mode shape at 6.75 hertz, modal participating mass of 16.8%, and scale factor of 75.

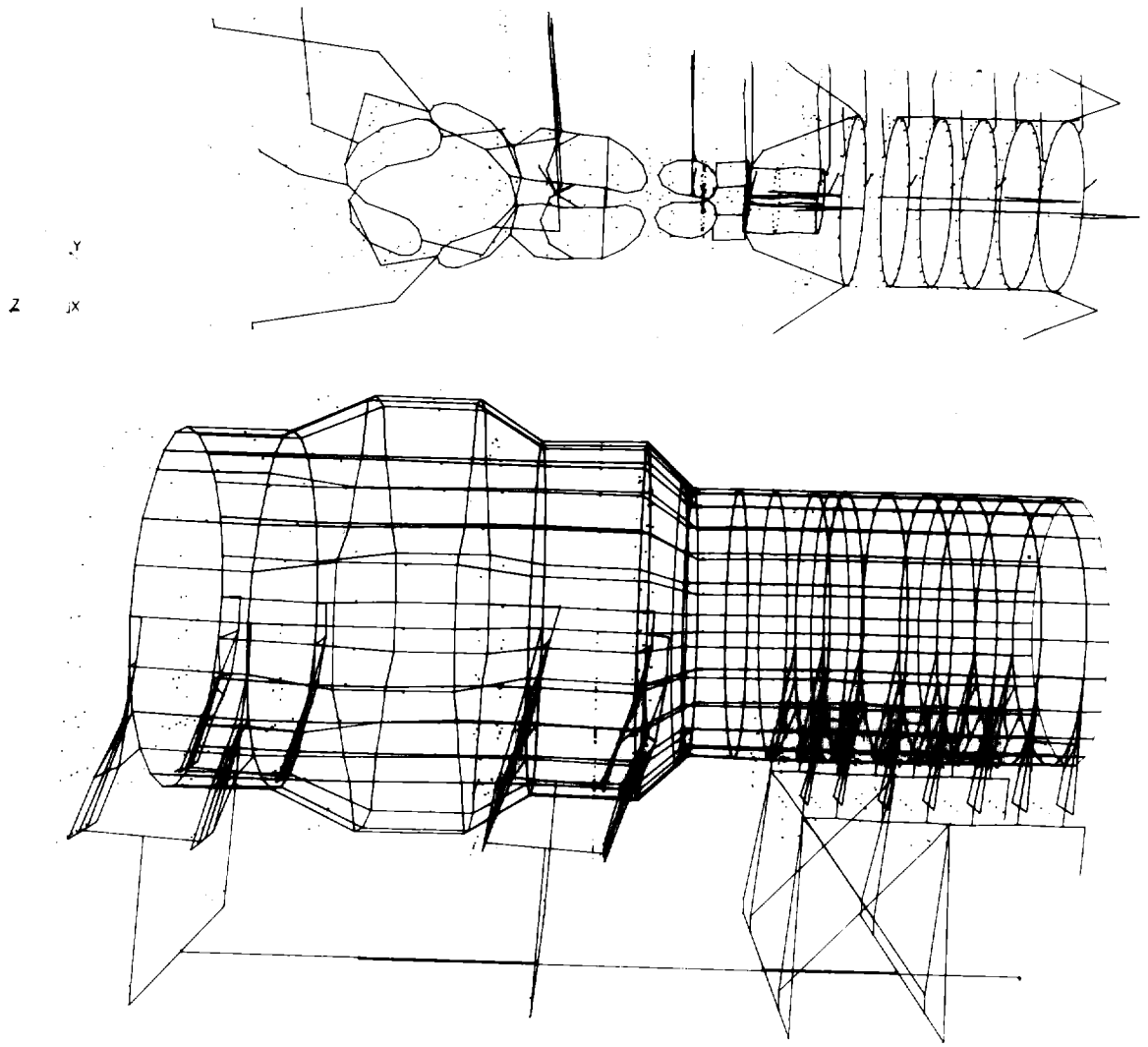

Figure 7. Computer model of magnet and vessel systems of MFTF-B Axicell: Longitudinal dominant-mode shape at 4.38 hertz, modal participating mass of 76.6%, and scale factor of 75.